A GROUNDMASS COMPOSITION FOR EET 79001A USING A NOVEL MICROPROBE TECHNIQUE FOR ESTIMATING BULK COMPOSITIONS. LITHOLOGY A AS AN IMPACT MELT? J. H. Jones[1] and, B. Z. Hanson[2]. [1]KR, NASA/JSC, Houston, TX 77058 (john.h.jones@nasa.gov), [2]Mail Code: SPFR-01-8, Corning Inc., Corning, NY 14831 (hansonbz@corning.com).

Introduction: Petrologic investigation of the shergottites has been hampered by the fact that most of these meteorites are partial cumulates. Two lines of inquiry have been used to evaluate the compositions of parental liquids: (i) perform melting experiments at different pressures and temperatures until the compositions of cumulate crystal cores are reproduced [e.g., 1]; and (ii) use point-counting techniques to reconstruct the compositions of intercumulus liquids [e.g., 2].

The second of these methods is hampered by the approximate nature of the technique. In effect, element maps are used to construct mineral modes; and average mineral compositions are then converted into bulk compositions. This method works well when the mineral phases are homogeneous [3]. However, when minerals are zoned, with narrow rims contributing disproportionately to the mineral volume, this method becomes problematic. Decisions need to be made about the average composition of the various zones within crystals. And, further, the proportions of those zones also need to be defined.

We have developed a new microprobe technique to see whether the point-count method of determining intercumulus liquid composition is realistic. In our technique, the approximating decisions of earlier methods are unnecessary because each pixel of our x-ray maps is turned into a complete eleven-element quantitative analysis.

The success or failure of our technique can then be determined by experimentation. As discussed earlier, experiments on our point-count composition can then be used to see whether experimental liquidus phases successfully reproduce natural mineral compositions.

Regardless of our ultimate outcome in retrieving shergottite parent liquids, we believe our pixel-by-pixel analysis technique represents a giant step forward in documenting thin-section modes and compositions.

For a third time, we have analyzed the groundmass composition of EET 79001, 68 [Eg]. The first estimate of Eg was made by [4] and later modified by [5], to take phase diagram considerations into account. The Eg composition of [4] was too olivine normative to be the true Eg composition, because the ,68 groundmass contains no forsteritic olivine. A later mapping by [2] basically reconfirmed the modifications of [5]. However, even the modified composition of [5] has olivine on the liquidus for ~50°C before low-Ca pyroxene appears [6].

Our present, third, analysis of ,68 yields a composition that is somewhat different from previous attempts.

Analytical: Analyses were performed on EET 79001, 68 using a JEOL 8500F FEG electron microprobe. Beam conditions were 30 nA at 20 KeV defocused to 2µ. This accelerating voltage was chosen to minimize Na mobility. Five groundmass areas were analyzed. Each area contained 250 x 250 analyses, separated by 5µ intervals. Analytical time on each point was 0.5 sec. Total mapping time was ~48 hours.

Quantification of the map data (gross counts/second/nA) was based on several dozen fully quantitative analyses of each of the different phases present. Approriate standards were chosen that minimized matrix corrections and resulted in optimum accuracy.

Once these calibrating analyses were performed, the procedure is as follows: (i) Simple linear regressions of *gross count rate* vs. K-ratios (net count rate ratio of unknown-to-standard multiplied by the standard composition) were calculated. (ii) Systematic relationships between ZAF values (i.e., matrix corrections calculated for each element in each analysis) and K-ratios were determined empirically. For example, the Ca ZAF parameter varied systematically with the Fe K-ratio and was fit with a second order polynomial for all phase**s**. Therefore, each ZAF correction was related back to some elemental K-ratio, which is linearly related to gross counts. In the example given, the Ca ZAF is calculated from the gross Fe count rate. (iii) The raw map data were then corrected for dead time, normalized to current and count time. (iv) The linear regressions based on the quantitative analyses were used to calculate K-ratios for each pixel, then (v) an appropriate ZAF was applied to each element in each pixel based on the empirical K-ratio-ZAF relationships determined from the quantitative data. After the maps were quantified, specific pixels on all

Table 1: Estimated Eg Compositions

	McS & J	Longhi & Pan	Herd et al.	This Work
SiO_2	49.2	50.7	49.0	50.9
TiO_2	0.78	0.9	1.7	0.52
Al_2O_3	6.44	7.10	7.4	10.4
FeO	18.5	18.7	18.4	14.4
MnO	0.51	0.52	0.52	0.40
MgO	14.4	12.2	11.5	11.8
CaO	7.96	8.7	9.2	8.9
Na_2O	0.97	1.1	0.9	1.7
P_2O_5	0.75	—	1.2	0.6
Sum	=100	=100	=100	99.99
Mg#	58	54	55	59

phases were re-analyzed quantitatively as a check of the success of the empirical quantification scheme. All analyses agreed well within the precision of the analyses.

Thus, each pixel (analysis point) is a complete, quantitative chemical analysis. The 1σ error on our bulk analysis is ~1 wt.%. Our reported bulk analysis includes all analyses within ± 3σ of 100%.

Results: Table 1 summarizes the various Eg estimates, in chronological order from left to right. The Herd et al. and Longhi and Pan reconstructions of Eg are very similar [2, 5]. The main differences between this work and those of [2] and [5] are lower FeO and higher SiO_2, Al_2O_3 and Na_2O. In the latter cases, most of the differences can be explained by a slightly greater proportion of maskelynite than had been found previously.

The composition shown above excludes very high- and very low-sum analyses that are almost always associated with analyses on cracks and fractures. This composition is the average of the results from the five different areas that were individually analyzed. The standard deviations for these average concentrations are typically excellent.

Figure 1

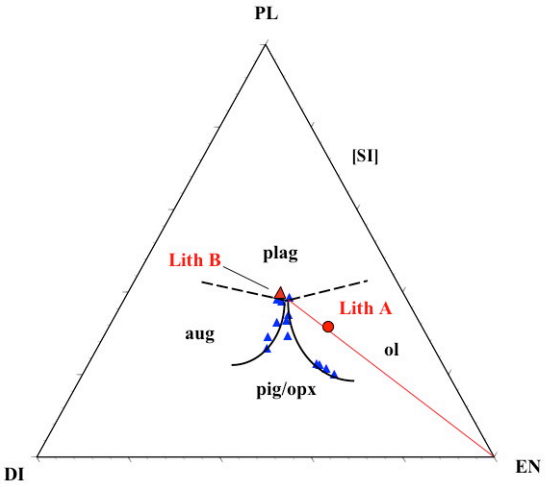

Figure 1. DI-PL-EN pseudo-ternary. Our new Eg composition (Lith A) falls on a mixing line between Lith B bulk [7] and an olivine-orthopyroxene mixture that plots at the EN corner. See text for discussion.

Discussion: Our new results are distinctly different from earlier estimates of the Eg composition. Most of the differences can be attributed to a greater proportion of modal maskelynite. But since all studies have included the same thin section of Lith A [79001,68], this difference between ours and other studies is likely not due to sample heterogeneity. And although we have great confidence in our analytical technique, this change from previous studies is unlikely to increase the frequency of maskelynite sampling.

We suspect the main difference between our study and that of Herd et al. [2] is the spatial sampling. Both studies acquired ~320,000 data points. However, Herd et al. sampled a larger area (6 mm x 22 mm) than the current study (6 mm x 6 mm). For an interstitial phase such as maskelynite, this difference in sampling (i.e., pixel size) may be crucial.

Figure 1 shows our new Eg composition (Lith A) plotted on the DI-PL-EN pseudoternary (red circle). Experimentally-determined phase boundaries and the composition of Lith B (red triangle) are shown for comparison. The olivine-low-Ca-pyroxene peritectic is from the study of [6] using the Eg composition of [5]; and the pigeonite-augite cotectic is from [1]. The Lith B composition is from [7].

Contrary to our expectations, our new Eg composition falls on no phase boundary. We had anticipated that our new result would be similar to that of [5], but would probably be less olivine normative. This is not the case.

The red line in Figure 1 is a mixing line between the minimum melt composition in the DI-PL-EN system (approximated by Lith B) and the EN endmember of the ternary. Because of the projection from SI, both low-Ca pyroxene and olivine plot at this location. Our Eg composition falls on this mixing line. The observation that Lith A plots far from any phase boundary and, instead, lies on a mixing line, suggests a complex petrologic history.

Mittlefehldt et al. [8] have proposed that Lithology A is an impact melt and that a super-heated melt resembling Lith B assimilated harzburgitic or lherzolitic materials. Our new data certainly support such a model (~20% harzburgite addition), although difficulties remain. In particular, it is difficult to understand why an impact melt (Lithology A) and a microgabbroic basalt (Lithology B) should have, within error, the same crystallization age [9]. Further, our new composition still plots in the olivine field, even though Lithology A contains no olivine in its groundmass.

References: [1] Stolper E.M. and McSween H.Y., Jr. (1979) *GCA* **43**, 1475-1498. [2] Herd C.D.K. et al. (2002) *MAPS* **37**, 987-1000. [3] Maloy A.K. and Treiman A.H. (2007) *Am. Min.* **92**, 1781-1788. [4] McSween H.Y., Jr. and Jarosevich E. (1983) *GCA* **47**, 1501-1513. [5] Longhi J. and Pan V. (1989) *Proc. LPSC 19th*, 451-464. [6] Wasylenki L. et al. (1993) *Lunar Planet Sci. XXIV*. pp. 1491-1492. [7] Warren P.H. et al. (1999) *GCA* **63**, 2105-2122. [8] Mittlefehldt D.W., Lindstrom D.J., Lindstrom M.M., and Martinez R.R. (1999) *MAPS* **34**, 357-367. [9] Wooden J. et al. (1982) *Lunar Planet Sci. Conf. XIII*. pp. 879-880.